

# Multifunctional induction coil sensor for evaluation of carbon content in carbon steel

Yujue Wang<sup>1,2</sup>, Yevgen Melikhov<sup>1,3</sup>, *Member, IEEE*, and Turgut Meydan<sup>1,&</sup>, *Member, IEEE*

<sup>1</sup>Wolfson Centre for Magnetics, School of Engineering, Cardiff University, Cardiff, UK

<sup>2</sup>Faculty of Materials and Manufacturing, Beijing University of Technology, Beijing, China

<sup>3</sup>Institute of Fundamental Technological Research PAS, Pawinskiego 5B, 02-106, Warsaw, Poland

&Deceased

Carbon steel has proven to be an important structural and functional material that plays an irreplaceable role in the worldwide economy. The influence of carbon on the mechanical and magnetic properties of the steel is well understood. Thus, the precise knowledge of the amount of carbon content in steel is crucial. Magnetic Barkhausen noise (MBN), magnetic hysteresis loop (MHL) and impedance measurements are reliable tools to assess carbon content. In this work, a multifunctional induction coil sensor used for MBN, MHL and impedance measurements is designed and optimised. A multifunctional measurement system using the optimised induction coil is employed to measure MBN, MHL and impedance signals. The parabolic dependence of the maximum value of MBN envelope on carbon content in steel is theoretically analysed and experimentally verified. Coercive field and remanence from MHL measurements as well as the maximum impedance value are found to be proportional to carbon content and their dependence is explained with analytical simulations.

*Index Terms*—Carbon content, Impedance, Magnetic Barkhausen Noise, Magnetic Hysteresis Loop, Multifunctional sensor.

## I. INTRODUCTION

Carbon steel, with its wide usage, has proven to be an important structural and functional material that plays an irreplaceable role in the worldwide economy with applications ranging from heavy industry through transportation to construction. The influence of carbon on the mechanical and magnetic properties of the steel is well understood. In commercial carbon steel, which usually contains less than 1% carbon in weight, the most common phases or constituents are ferrite and pearlite (a lamellar microstructure mixed with ferrite and cementite) [1]. Ferrite shows high ductility, low hardness values and also general low magnetic hardness, while pearlite on the other hand shows much more brittle and higher mechanical and magnetic hardness [2]. The relative volume fraction of the ferrite and pearlite phases gives rise to the final properties of the steel. Thus, the precise knowledge of the amount of carbon content in steel is crucial.

Magnetic Barkhausen noise (MBN) method is sensitive to the microstructure of ferromagnetic material. Thus, the metallographic phase of steel related to carbon content would influence the Barkhausen emission, and inversely, MBN could be used to evaluate the amount of carbon in steel. However, since various MBN sensors were used to assess the carbon contents in steel, the comparison of results reported by different investigators appeared to conflict with each other. For example, Batista *et al.* [2] inserted the tested steels inside an electromagnet for MBN measurements and found the existence of two peaks of MBN profile. One of the peak amplitudes decreased with increasing amount of carbon from 0 wt% to 1.5 wt%, while the other one increased. But Samimi *et al.* [3] used a flux-controlled MBN system and located the MBN sensor on top of the surface of tested steels. They experimentally observed just one peak of MBN envelope in half excitation cycle, and the peak amplitude increased with the increase in the

amount of carbon, but it abruptly dropped when the carbon content exceeded 0.65 wt%. Either one peak or two peaks of MBN envelope for carbon steel evaluation were found by other investigators [4,5], but the height of peaks was not correlated with the carbon content in steel.

Besides, MBN signal is the voltage pulses induced in the pick-up coil by the change of discrete micromagnetic flux caused by the irreversible movement of magnetic domain walls during the cyclic magnetisation process. It has been observed that the MBN signal strongly depended on the measurement parameters such as magnetising frequency [6], and the resonant frequency of pick-up coil [7], which widely varied from one MBN system to another. It resulted in an inconsistent correlation between microstructural variations and MBN signals in different investigations. Therefore, it was considerable to optimise the MBN pick-up coil for the assessment of the relative amount and contributions of the carbon in steels.

Magnetic hysteresis loop (MHL) is another widely used magnetic technique for the microstructure characterisation of ferromagnetic materials [8]. Hysteresis measurements could provide reproducible and reliable results. But it was only appropriate for the samples with a special shape like cylinder that could be wound coils to measure the magnetic induction [2]. There were various magnetic properties that can be extracted from the hysteresis loop, like the coercive field, remanence, and differential permeability. Jiles *et al.* [8], and Thompson *et al.* [9] found that the coercive field of the hysteresis loop increased linearly with the increasing carbon content in steel.

The interaction between induction coil and the tested steel would change the electrical properties of coil, such as impedance. Davis *et al.* [10] used this characteristic estimated the fraction of ferrite in dual phase steel accurately. Hence, the electrical properties could also be a potential method to evaluate

the carbon volume in steel.

In this work, to improve the accuracy of carbon content evaluation, a multifunctional induction coil sensor used for MBN, MHL and impedance measurements is designed and optimised. Besides, a multifunctional measurement system using the optimised induction coil is built to measure the various signals. Furthermore, the measured results are theoretically analysed and discussed.

## II. THE OPTIMISATION OF INDUCTION COIL

The induction coil, composed of a multilayer solenoid coil wound on the tested steel, is usually made of enamelled wire, which introduces inductance (L), parasitic capacitance (C) and resistance (R) to the measurement system. These parasitic elements will determine the resonant frequency, sensitivity, and signal-to-noise ratio (SNR) of MBN sensor.

### A. Inductance

Maxwell gave an expression for the mutual inductance of hypothetical filaments, which had finite length but zero cross-sectional area and were spaced at the Geometric Mean Distance (GMD), in complete elliptic integrals. It was further improved by [11]:

$$M = \mu_c \sum_{i=1}^{N_{tot}} \sum_{j=1, j \neq i}^{N_{tot}} \sqrt{(r_i + r_j)^2 + s_{ij}^2} \left[ (1 - \varepsilon_{ij}^2 / 2) F(k_{ij}) - E(k_{ij}) \right] \quad (1)$$

where  $\mu_c$  is the relative magnetic permeability of the core,  $N_{tot}$  is the total number of turns of coil,  $r$  is the distance between wire centre and axial centre,  $s$  is the distance between two wires,  $\varepsilon$  is the elliptic integral modulus,  $F$  and  $E$  are complete elliptical integrals of first and second kinds, respectively.

The self-inductance could be calculated by

$$L_s = \mu_c \sum_{i=1}^{N_{tot}} (2r_i - r_w) \left[ (1 - \varepsilon_i^2 / 2) F(k_i) - E(k_i) \right] \quad (2)$$

where  $r_w$  is the radius of a wire. And the total inductance of the multilayer solenoid coil was obtained by the superposition of  $L_s$  and  $M$  contributions as

$$L = M + L_s \quad (3)$$

### B. Capacitance

The total value of the self-capacitance in multilayer solenoid coils with ferromagnetic core includes the following four parts: the turn-to-turn capacitances ( $C_{tt}$ ), the layer-to-layer capacitances ( $C_{ll}$ ), the outer-layer capacitances ( $C_{ol}$ ) and the turn-to-core capacitances ( $C_{tc}$ ) as shown in Fig.1.

## FIG. 1 HERE

The inner surface and the external surface of coating form a dielectric capacitance. The elementary capacitance related to the cylindrical coating shell  $dC_i$  is given by[12]

$$dC_i = \varepsilon_r \varepsilon_0 \int_0^{l_i} dl \int_{d_0/2}^{d_c/2} r / dr = \frac{\varepsilon_r \varepsilon_0 l_i}{\ln(d_0 / d_c)} d\theta \quad (4)$$

where  $\varepsilon_0$  is the vacuum permittivity,  $\varepsilon_r$  is the relative permittivity of the insulation coating,  $d_0$  is the diameter of the

wire,  $d_c$  is the copper core, and  $l_i$  is the length of a turn.

Similarly, the elementary capacitance induced by the air gap  $dC_g$  per unit angle can be calculated by

$$dC_g = \frac{\varepsilon_r \varepsilon_0 l_i}{2l_g} d\theta = \frac{\varepsilon_r \varepsilon_0 l_i d\theta}{2[d_0(1 - \cos \theta) + \xi_T]} \quad (5)$$

The turn-to-turn capacitance  $C_{tt}$  is equal to the layer-to-layer capacitance  $C_{ll}$ , which is composed of the series combination of three elementary capacitances

$$C_{tt} = C_{ll} = \int_{-\pi/6}^{\pi/6} \frac{\varepsilon_0 l_i d\theta}{2 \left( 1 + \frac{1}{\varepsilon_r} \ln \frac{d_0}{d_c} - \cos \theta \right)} \quad (6)$$

Similarly,  $C_{ol}$  and  $C_{tc}$  can be calculated by the same way. And the total stray capacitance of the hexagonal winding coil is given by

$$C_s = \frac{1}{N_{tot}} [(N_T - 1) N_L C_{tt} + \sum_{i=1}^{2N_T - 1} i^2 (N_L - 1) C_{ll} + (N_L + N_T - 2) C_{ol} + (2N_T - 1)^2 (N_L - 1) C_{ol} + \sum_{j=1}^{N_L} j^2 C_{tc}] \quad (7)$$

where  $N_T$  is the turns per layer and  $N_L$  is the number of layers.

### C. Optimisation of induction coil

It is known that the MBN profile strongly depends on the resonant frequency characteristics of the pickup coil. The optimised coil could be the basis for studying microstructure in ferromagnetic material like metallographic phases in steel. Its resonant frequency of induction coil  $f_0$  can be given by

$$f_0 = \frac{1}{2\pi\sqrt{LC}} \sqrt{1 - \left( \frac{R^2 C}{4L} \right)} \quad (8)$$

To obtain an intensive output signal and good signal-to-oise ratio (SNR), the outer diameter of coil  $D_o$  and length of coil  $l$  is recommended to be about four times the ferromagnetic core and 0.7~0.9 of the length of the core, respectively [13]. Additionally, The lengths and diameters of all tested samples are the same and determined as 50 mm and 8 mm, respectively. Moorthy [8] found that it was important to use an MBN sensor with a good response in a low frequency range of less than 10 kHz to detect MBN signals from the deep subsurface effectively. Under these limited conditions, three Standard Wire Gauge (SWG) grades 25, 29 and 35 wires with 0.48 mm, 0.33 mm and 0.200 mm diameters of copper cores respectively are used to optimise the pick-up coil size.

## III. MULTIFUNCTIONAL INDUCTION COIL AND MEASUREMENT SYSTEM

### A. Multifunctional induction coil

The multifunctional induction coil is used to measure MBN, MHL and impedance signals. It is wound on the tested cylindrical samples in this study, So the coil is a ferromagnetic core sensor. Due to the small diameter of SWG-35 wire, it requires large amounts of turns (more than 22000 turns) to meet the limited conditions of coil sizes. For SWG-25 wire, the reverse applies. As it does not need abundant turns to wind the coil in defined sizes, the resonant frequencies of the coils made by SWG-25 wires are much higher than 10 kHz. Therefore, the

optimised sizes of the induction coil made by SWG-29 wires are determined as 8 mm in inner diameter, 32 mm in outer diameter, and 35.2 mm in length, respectively, for saving turns, weight and closing to the required resonant frequency.

The optimised MBN pick-up coil is tailored by Anstee Coil Technology Ltd. using self-bonding enamelled copper wire SWG-29 (4225 turns). Agilent 4294A precision impedance analyser is used to measure the tailored coil. The value of coil (107.9141 mH, 66.9512 pF) calculated by the introduced model for air core coil is close to the manufactured (108.8930 mH, 67.9956 pF).

### B. Measurement system

The experimental set-up used for carbon content measurements is shown in Fig. 2. The laboratory C-core with tapered poles electromagnet can generate an intense magnetic field with low frequency. It can work on quasi-static frequency by being fed in correlative current from a computer-controlled bipolar power supply. The tapered poles can be driven by an adjustable lever to match the length of sample.

During the MBN and MHL measurements, A sinusoidal voltage waveform of 0.5Hz generated by the computer is amplified by the bipolar power supply. The feeding current from the bipolar power supply into the electromagnet generates the corresponding magnetic field. The coil can detect the MBN emissions, magnetic flux density and impedance. A data acquisition card USB-6366 is used to measure MBN signals with a sampling rate of 1 MS/s. The strength of applied magnetic field  $H$  is measured at the surface of the sample by a transverse Lakeshore Hall probe. The impedance is independently measured by impedance analyser.

**FIG. 2 HERE**

### C. Carbon steel samples

There are various samples examined in this study, including a high purity iron (iron content > 99.99%) and different kinds of carbon steels containing carbon from 0.085% to 0.81% in weight as listed in Table 1. These samples are machined into cylindrical shapes with the same diameter and length of 8 mm and 50 mm, respectively. Besides, to verify the methodology, another carbon steel graded 080M40 (with 0.46% carbon content) is further measured using the same experimental setup and induction coil.

**TABLE 1 HERE**

## IV. RESULTS AND DISCUSSION

### A. Magnetic Barkhausen Noise

The cylindrical samples are magnetised along their axial

direction by a sinusoidal magnetic field maximum strength of 11,000 A/m at excitation frequencies of 0.5 Hz. Fig. 3 shows the MBN raw signals and smoothed envelopes for pure iron, 1055 and 1075 grades steels.

**FIG. 3 HERE**

Generally, the pinning effect in magnetic domains is caused by non-ferromagnetic elements, of which carbon is the most abundant component. Carbon exists in Fe-C alloys in the form of compounds or interstitial solid solutions, and its presence hinders the inversion of magnetic domains. Assuming that the morphology of carbon element in carbon steel is a three-dimensional sphere, the number of MBN signal is usually related to the volume and content of carbon element.

Coercivity is related to the number of pinning and the local magnetic field  $H_0$  at the pinning point. The local magnetic field is also called the critical magnetic field, that is, the magnetic field required by the domain wall to overcome the pinning effect and produce the domain wall displacement. Due to the correlation between magnetic Barkhausen noise signal and coercivity which is determined by the pinning number and local magnetic field, MBN signal can be expressed as [15]

$$M_{\max} \sim \frac{1}{G}(H - H_c) \sim \frac{1}{G} \left( H - \left( \frac{\pi}{2} \left( \frac{6}{\pi} \right)^{\frac{5}{3}} \cdot \frac{K}{I_s} \cdot \frac{\delta}{d^4} \right) w_c^{\frac{5}{3}} \right) \quad (9)$$

where  $G$  is a constant,  $H$  is magnetic field,  $H_c$  is the coercive field,  $K$  is the anisotropic coefficient,  $I_s$  is the spontaneous magnetization,  $\delta$  is the thickness of domain wall,  $d$  is the diameter of carbon and  $w_c$  is the content of carbon. Equation (9) shows that there is a 5/3-fold relationship between the peak characteristics of MBN and the carbon content, which can be approximated as a square relationship. It can be found in Fig. 3d that the parabolic function could better approximate the experimental results with fitting goodness  $R^2$  higher than 0.94. Besides, it can be found that the relative error between mathematical function and the verified point (red cross) of 080M40 is 5.51%, which indicates MBN peak value could be a potential parameter to evaluate the carbon content in steels.

### B. Magnetic Hysteresis Loop

The magnetic hysteresis loops of pure iron, 1055 and 1075 grades of steel are plotted in Fig. 4a. It is clearly shown that the hysteresis loop is broadening with the increasing carbon content of steel.

For dual-phase ferromagnetic materials, the hysteresis J-A model combined with Boltzmann transition function is used for modelling their hysteresis loops. In the simulation of hysteresis loop of dual-phase material based on J-A model, two sets of hysteresis parameters are set, and then the transition between two single phases is realized by Boltzmann function, which is expressed as [16]

$$y = \frac{A_1 - A_2}{1 + e^{(|H| - H_{ex})/\Delta H}} + A_2 \quad (10)$$

where  $y$  is the hysteresis parameters of transition dual-phase,  $A_1$  and  $A_2$  are the hysteresis parameters of ferrite and pearlite phases. Coercivity is an important parameter on hysteresis loop. Its transition characteristics can also be described by Boltzmann function. Though Boltzmann function is nonlinear, in the analysis range (carbon content from 0% to 0.8%), the coercivity calculated by Boltzmann function can be approximate to a linear function. The dependency of the coercivity on carbon content in steels is shown in Fig. 4b. It shows the coercivity increases as a linear function of carbon content with a coefficient of determination higher than 0.97. Besides, it can be found that the relative errors between mathematical function and the verified point of 080M40 is 5.38%, which indicates coercivity could be another potential parameter to evaluate the carbon content in steels.

**FIG. 4 HERE**

### C. Impedance measurement

The impedance of various grades of steel are plotted in Fig. 5a. It is clearly shown that the impedance is increasing with the increasing carbon content of steel. The dependency of the impedance  $Z$  on carbon content in steels presents linearly increase trend as shown in Fig. 5b.

Empirically based power law model is popularly used. The power law model predicts the effective permeability as [10]

$$\mu_e = (1-f)\mu_1^\beta + f\mu_2^\beta \quad (11)$$

Where  $\mu_1$  and  $\mu_2$  are the relative permeability values of the first and second phase respectively,  $f$  is the fraction of the second phase, and  $\beta$  is a dimensionless parameter. It indicates the impedance peak value should present a linear correlation with carbon content. Though the measured result of 080M40 for impedance maximum value deviate from the linear fitting function as shown in Fig. 5b, the coefficient of determination for the linear function fitted by other points is higher than 0.95. Therefore, comprehensively using three indicators could improve the accuracy of the evaluation of the carbon content in steels.

**FIG. 5 HERE**

## V. CONCLUSION

This paper discussed the optimisation steps for the multifunctional induction coil based on the inductance and stray capacitance models. The comparison of the designed coil and the manufactured coil according to optimised size verified the feasibility of the optimisation method.

The MBN, MHL and impedance experiments were conducted to analyse the dependency of these signals on the amount of carbon in steel using the optimised multifunctional

induction coil. The peak value of MBN envelope was experimentally and theoretically observed as a parabolic function of carbon content. The multifunctional measurement system was also used to obtained magnetic hysteresis loops of various steels. The coercivity presented linear dependence on the amount of carbon in steel, which was corresponding to the model. At last, the impedance of coil was measured when inserting different samples. The peak value of impedance also presented a linear increase with the increase of carbon level.

## ACKNOWLEDGMENT

This work was supported by Cardiff University and China scholarship council (CSC).

## REFERENCES

- [1] H. Okamoto, "The C-Fe (carbon-iron) system," *J. Phase Equilibria*, vol. 13, pp. 543–565, 1992.
- [2] L. Batista, U. Rabe, I. Altpeter, et al., "On the mechanism of nondestructive evaluation of cementite content in steels using a combination of magnetic Barkhausen noise and magnetic force microscopy techniques," *J. Magn. Magn. Mater.*, vol. 354, pp. 248–256, 2014.
- [3] A. A. Samimi, T. W. Krause, and L. Clapham, "Multi-parameter Evaluation of Magnetic Barkhausen Noise in Carbon Steel," *J. Nondestruct. Eval.*, vol. 35, pp. 1–8, 2016.
- [4] J. A. Pérez-Benitez, J. Capó-Sánchez, J. Anglada-Rivera et al., "A model for the influence of microstructural defects on magnetic Barkhausen noise in plain steels," *J. Magn. Magn. Mater.*, vol. 288, pp. 433–442, 2005.
- [5] S. Zhang, X. Shi, L. Udpa, and Y. Deng, "Micromagnetic measurement for characterization of ferromagnetic materials' microstructural properties," *AIP Adv.*, vol. 8, pp. 056614 (1-7), 2018.
- [6] A. Dhar and D. L. Atherton, "Influence of magnetising parameters on the magnetic Barkhausen noise," *IEEE Trans. Magn.*, vol. 28, pp. 3363–3366, 1992.
- [7] V. Moorthy, "Important factors influencing the magnetic Barkhausen noise profile," *IEEE Trans. Magn.*, vol. 5, pp. 1–13, 2015.
- [8] D. C. Jiles, J. B. Thoeke, and M. K. Devine, "Numerical determination of hysteresis parameters for the modeling of magnetic properties using the theory of ferromagnetic hysteresis," *IEEE Trans. Magn.*, vol. 28, pp. 27–35, 1992.
- [9] S. M. Thompson and B. K. Tanner, "The magnetic properties of pearlitic steels as a function of carbon content," *J. Magn. Magn. Mater.*, vol. 123, pp. 283–298, 1993.
- [10] L. Zhou, R. Hall and C.L. Davis, "Measured and modelled low field relative permeability for dual phase steels at high temperature," *J. Magn. Magn. Mater.*, vol. 475, pp. 38–43, 2019.
- [11] J. Martínez, S. Babic, and C. Akyel, "On evaluation of inductance, DC resistance, and capacitance of coaxial inductors at low frequencies," *IEEE Trans. Magn.*, vol. 50, pp. 1–12, 2014.
- [12] B. Wu, X. Zhang, X. Liu, et al., "An analytical model for predicting the self-capacitance of multi-layer circular-section induction coils," *IEEE Trans. Magn.*, vol. 54, pp. 1–7, 2018.
- [13] W. Richter, "Induktionsmagnetometer für biomagnetische Felder," *Exp. Tech. Phys.*, vol. 27, pp. 235–243, 1979.
- [14] L. Clapham, C. Jagadish, and D. L. Atherton, "The influence of pearlite on Barkhausen noise generation in plain carbon steels," *Acta Metall. Mater.*, vol. 39, pp. 1555–1562, 1991.
- [15] H. Sakamoto, M. Okada and M. Homma, "Theoretical analysis of Barkhausen noise in carbon steels," *IEEE Trans. Magn.*, vol. 23, pp. 2236–2238, 1987.
- [16] A. Raghunathan, Y. Melikhov, J. E. Snyder, and D. C. Jiles, "Modeling of two-phase magnetic materials based on Jiles-Atherton theory of hysteresis," *J. Magn. Magn. Mater.*, vol. 324, pp. 20–22, 2012.

**Table 1. Carbon analysis results**

Samples	Pure iron	230M07	1015	1045	1055	1075
Carbon [%]	<0.001	0.085	0.190	0.480	0.600	0.810

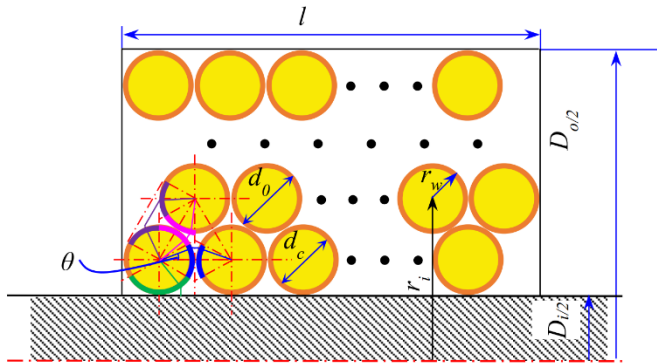


**FIG. 1** Schematic diagram of the hexagonal winding coil (blue pair line represents the turn-to-turn capacitance, magenta pair line represents the layer-to-layer capacitance, purple pair line represents the outer-layer capacitance and green pair line represents the turn-to-core capacitance).

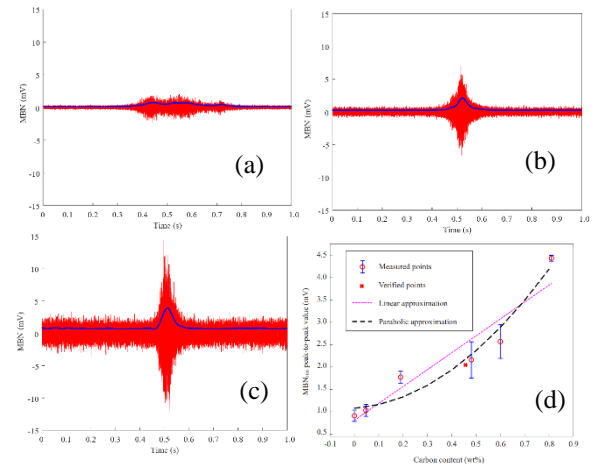


**FIG. 3** Barkhausen voltage bursts acquired for (a) pure iron, (b) 1055, (c) 1075 and (d) MBN peak value as function of carbon content.

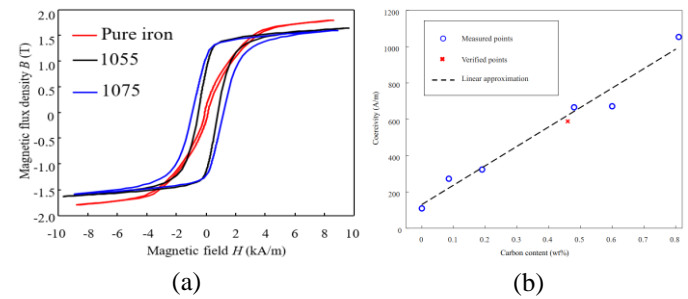


**FIG. 4** (a) Magnetic hysteresis loops carbon steel and (b) coercivity as a linear function of carbon content.

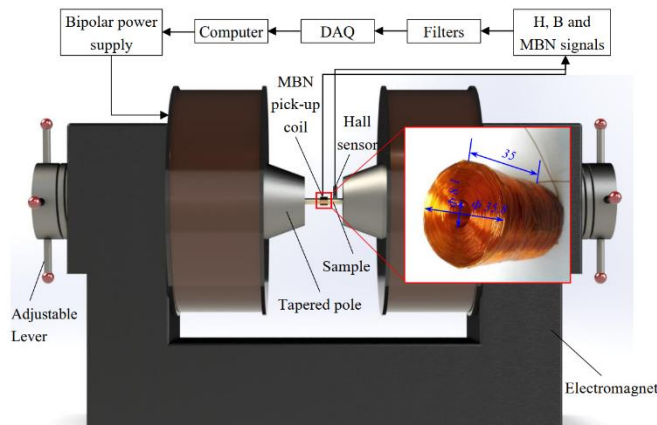


**FIG. 2** The multifunctional measurement system.

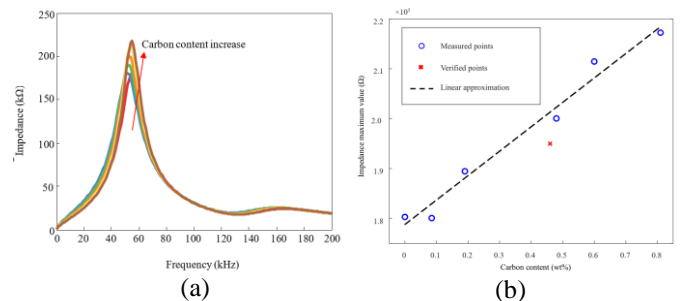


**FIG. 5** (a) The impedance as function of frequency and (b) impedance peak value as linear function of carbon content.